Inorganic Chemistry
Article

Inorg. Chem. **2009**, *48*, 11451–11458 **11451**
DOI: 10.1021/ic9016883

Vibrioferrin, an Unusual Marine Siderophore: Iron Binding, Photochemistry, and Biological Implications

Shady A. Amin,[†] David H. Green,[‡] Frithjof C. Küpper,[‡] and Carl J. Carrano*[,†]

[†]*Department of Chemistry and Biochemistry, San Diego State University, San Diego, California 92182-1030, and* [‡]*Scottish Association for Marine Science, Dunstaffnage Marine Laboratory, Oban, Argyll PA37 1QA, Scotland, U.K.*

Received August 25, 2009

Vibrioferrin (VF) is a member of the carboxylate class of siderophores originally isolated from *Vibrio parahaemolyticus*, an enteropathogenic estuarine bacterium often associated with seafood-borne gastroenteritis. Recently we have also isolated this siderophore from several species of *Marinobacter*, which are closely associated or "symbiotic" with toxic, bloom-forming dinoflagellates such as *Gymnodinium catenatum*. We have measured the overall metal−ligand binding constant for iron-vibrioferrin (FeVF) as $10^{24.02(5)}$ making vibrioferrin one of the weakest iron chelators of any known marine siderophore. FeVF is also shown to be considerably more sensitive to photolysis under relatively low illumination conditions than other photoactive siderophores leading primarily to a monodecarboxylated photoproduct that has no significant affinity for Fe(III). The consequences that these features have on bacterial-algal interactions with potential importance to understanding the origin and sustenance of harmful algal blooms are discussed.

Introduction

Iron is an essential element for nearly all living organisms because of its ubiquitous role in redox enzymes, especially in the context of respiration and photosynthesis. However, although it is the fourth most abundant element in the Earth's crust, it is present under aerobic conditions at neutral pH only in the form of extremely insoluble minerals like hematite, goethite, and pyrite or as polymeric oxide-hydrates, -carbonates, and -silicates that severely restrict the bioavailability of this metal. The iron level in open ocean waters is even lower than in most terrestrial environments,[1] since a large fraction of the limited iron available is already tightly complexed (although the nature of the complexing ligands remains unknown).[1a,2] To deal with this low bioavailability, bacteria and fungi have evolved sophisticated systems based on high-affinity iron-specific binding compounds called siderophores to acquire, transport, and process this essential metal ion. Their major role is the extracellular solubilization of iron from minerals and/or organic substrates and its specific transport into microbial cells. Several hundred siderophores, whose biosyntheses are repressed by high iron levels, are known, and extensive studies of their isolation, structure, transport, and molecular genetics have been undertaken in the last three decades.[3] The structural variety of siderophores has been comprehensively reviewed.[4] However the study of marine siderophores is less extensive as compared to their terrestrial counterparts, and the structures of only a relatively few have been fully elucidated.[5] It is noteworthy that a large percentage of the characterized marine siderophores can be classified as amphiphilic, suggesting a different iron uptake strategy than that typically found in terrestrial microorganisms.[5a,c,6] In addition the presence of α- or β-hydroxy carboxylate groups in many marine siderophores renders their iron complexes photoactive.[7] It has been proposed that sunlight-driven photoreduction of the Fe(III) in such siderophores would transiently produce Fe(II) which might be utilizable by other organisms.[8]

*To whom correspondence should be addressed. E-mail: carrano@sciences.sdsu.edu.

(1) (a) Bruland, K. W.; Donat, J. R.; Hutchins, D. A. *Limnol. Oceanogr.* **1991**, *36*, 1555. (b) Martin, J. H.; Fitzwater, S. E. *Nature* **1988**, *331*, 341. (c) Wu, J.; Luther, G. W., III *Limnol. Oceanogr.* **1994**, *39*, 1119.

(2) (a) Gledhill, M.; van den Berg, C. M. G. *Mar. Chem.* **1994**, *47*, 41. (b) Vraspir, J. M.; Butler, A. *Annu. Rev. Mar. Sci.* **2009**, *1*, 43.

(3) Winkelmann, G.; Carrano, C. J.*Transition metals in microbial metabolism*; Harwood Academic Publishers: Amsterdam, 1997.

(4) Raymond, K. N. *Pure Appl. Chem.* **1994**, *66*, 773.

(5) (a) Martinez, J. S.; Carter-Franklin, J. N.; Mann, E. L.; Martin, J. D.; Haygood, M. G.; Butler, A. *Proc. Natl. Acad. Sci. U.S.A.* **2003**, *100*, 3754. (b) Martinez, J. S.; Haygood, M. G.; Butler, A. *Limnol. Oceanogr.* **2001**, *46*, 420. (c) Martinez, J. S.; Zhang, G. P.; Holt, P. D.; Jung, H. T.; Carrano, C. J.; Haygood, M. G.; Butler, A. *Science* **2000**, *287*, 1245. (d) Reid, R. T.; Livet, D. H.; Faulkner, D. J.; Butler, A. *Nature* **1993**, *366*, 455.

(6) Martin, J.; Ito, Y.; Homann, V.; Haygood, M.; Butler, A. *J. Biol. Inorg. Chem.* **2006**, *11*, 633.

(7) (a) Barbeau, K.; Rue, E. L.; Bruland, K. W.; Butler, A. *Nature* **2001**, *413*, 409. (b) Barbeau, K.; Zhang, G.; Live, D. H.; Butler, A. *J. Am. Chem. Soc.* **2002**, *124*, 378.

(8) Maldonado, M. T.; Strzepek, R. F.; Sander, S.; Boyd, P. W. *Global Biogeochem. Cycles* **2005**, 19.

Published on Web 10/12/2009

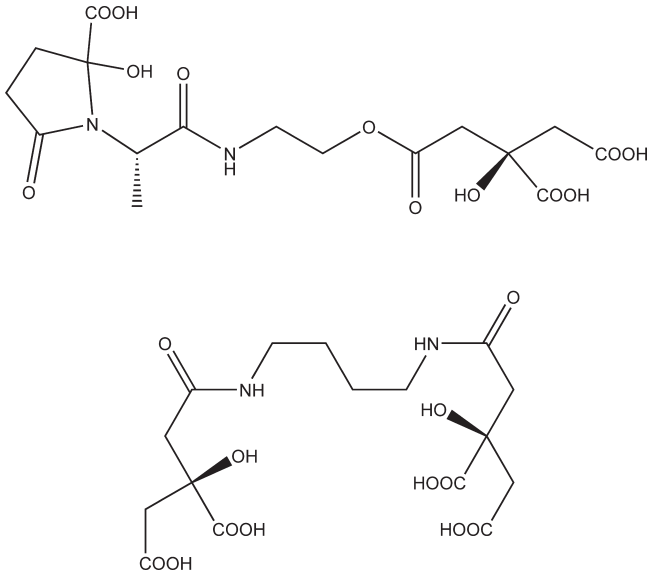

Figure 1. Structures of the siderophores vibrioferrin (top) and rhizoferrin (bottom).

However, it was subsequently shown that the photooxidized siderophore is still capable of rapidly rebinding the iron,[7a,9] and in the one case studied, transporting it into the cell of the producing bacteria.[9b]

Algal blooms are ubiquitous phenomena that have been increasingly observed in the coastal and upwelling parts of the world's oceans. Even in the absence of toxin production, these events often alter the chemical and ecological milieu by changing nutrient distribution and consequently the biodiversity of marine ecosystems. Although many physical and biological factors influence bloom dynamics, emerging evidence suggests that bacterial-algal interactions may be contributing to the development and sustenance of blooms.[10] Indeed, some bacterial associates of harmful algal species are clearly important to the physiological welfare of algal cells as evidenced by the fact that many such species including the dinoflagellate *Gymnodinium catenatum* cannot be grown axenically indicating an obligatory requirement(s) that is supplied by bacteria.[10] One attractive hypothesis concerning the nature of this interspecies interaction that we are pursuing is that phytoplankton can "share" iron, an element often limiting to their growth and previously shown to impact bloom formation,[11] bound to extracellular siderophores produced by their bacterial associates. Although some diatoms have been shown to assimilate iron bound to bacterial siderophores,[12] the iron acquisition systems of another important group of phytoplankton, the dinoflagellates, are for the most part unknown.[13]

Vibrioferrin (VF) is a member of the carboxylate class of siderophores and contains two α-hydroxy acid groups (Figure 1). It was originally isolated from *Vibrio parahaemolyticus*, an enteropathogenic estuarine bacterium often associated with seafood-borne gastroenteritis and has been extensively studied by Yamamoto et al.[14] Our interest in VF stems from the fact that we have also isolated this siderophore from several species of marine bacteria, including *Marinobacter spp*. DG870, 879, and 979 and *M. algicola* DG893, which are closely associated or "symbiotic" with toxic, bloom-forming dinoflagellates such as *G. catenatum*.[15] Despite the fact that VF has been extensively studied from a molecular biology perspective,[14a,d,e] its metal binding characteristics remain largely unknown. In this manuscript we describe the iron binding constants for this unusual siderophore and discuss how these, and its unexpected photochemical properties, are related to biological function.

Experimental Section

Siderophore Isolation. Vibrioferrin was isolated and purified as previously described.[15]

Potentiometric and Spectrophotometric Titrations. Standard carbonate-free solutions of NaOH were prepared from Baker "Dilut-It" ampules using boiled, purified water (i.e., 18 MΩ resistance; Milli-Q) and were stored under Ascarite scrubbed argon. Base solutions were standardized with KHP to the phenolphthalein end point. The absence of carbonate (< 2%) was confirmed by Gran's plots.[16] Iron solutions were purchased from Fluka ($FeCl_3 \cdot 6H_2O$ in 4% HCl) and the exact iron concentration determined by EDTA titration with Variamine Blue as an indicator.[9b] Excess acid in the iron solution was determined by passing an aliquot through a well-washed sample of the acid form of AG 50W-X8 cation exchange resin (Bio-Rad) and titrating the liberated acid. The excess acid was the difference between the total acid and three times the known iron concentration. Spectrophotometric and potentiometric titrations were performed in a foil covered, jacketed, three-necked titration vessel and connected to a constant temperature water bath held at 25.0(1)°C. Ionic strength was fixed at 0.1 M with NaCl. Hydrogen ion concentration was measured using a Mettler-Toledo DL50 titrator connected to a Mettler-Toledo DG111−5C combination electrode which was standardized with a three buffer sequence and corrected (as needed) to read the negative log of the hydrogen ion concentration directly using dilute HCl solutions. Titrant was added to the cell, which was kept under a blanket of Ascarite scrubbed argon gas. Ligand protonation constants were determined from the nonlinear refinement of the potentiometric titration data using the program BEST developed by Martell and Motekaitis while metal−ligand constants utilized HYPERQUAD.[17] Spectrophotometric titration

(9) (a) Abergel, R. J.; Zawadzka, A. M.; Raymond, K. N. *J. Am. Chem. Soc*. **2008**, *130*, 2124. (b) Küpper, F. C.; Carrano, C. J.; Kuhn, J.-U.; Butler, A. *Inorg. Chem*. **2006**, *45*, 6028.

(10) Kodama, M.; Doucette, G.; Green, D. Relationships Between Bacteria and Harmful Algae. In *Ecology of Harmful Algae*; Granéli, E., Turner, J. T., Eds.; Springer-Verlag: Heidelberg, 2006; pp 243−255.

(11) (a) Martin, J. H.; et al. *Nature* **1994**, *371*, 123. (b) Boyd, P. W.; et al. *Nature* **2000**, *407*, 695.

(12) Soria-Dengg, S.; Reissbrodt, R.; Horstmann, U. *Mar. Ecol.: Prog. Ser*. **2001**, *220*, 73.

(13) (a) Naito, K.; Imai, I.; Nakahara, H. *Phycol. Res*. **2008**, *56*, 58. (b) Naito, K.; Matsui, M.; Imai, I. *Harmful Algae* **2005**, *4*, 1021.

(14) (a) Funahashi, T.; Moriya, K.; Uemura, S.; Miyoshi, S.-I.; Shinoda, S.; Narimatsu, S.; Yamamoto, S. *J. Bacteriol*. **2002**, *184*, 936. (b) Takeuchi, Y.; Nagao, Y.; Toma, K.; Yoshikawa, Y.; Akiyama, T.; Nishioka, H.; Abe, H.; Harayama, T.; Yamamoto, S. *Chem. Pharm. Bull*. (*Tokyo*) **1999**, *47*, 1284. (c) Takeuchi, Y.; Akiyama, T.; Harayama, T. *Chem. Pharm. Bull*. (*Tokyo*) **1999**, *47*, 459. (d) Tanabe, T.; Funahashi, T.; Nakao, H.; Miyoshi, S.-I.; Shinoda, S.; Yamamoto, S. *J. Bacteriol*. **2003**, *185*, 6938. (e) Tanabe, T.; Nakao, H.; Kuroda, T.; Tsuchiya, T.; Yamamoto, S. *Microbiol. Immunol*. **2006**, *50*, 871. (f) Yamamoto, S.; Akiyama, T.; Okujo, N.; Matsu-ura, S.; Shinoda, S. *Microbiol. Immunol*. **1995**, *39*, 759. (g) Yamamoto, S.; Okujo, N.; Matsuura, S.; Fujiwara, I.; Fujita, Y.; Shinoda, S. *Microbiol. Immunol*. **1994**, *38*, 687. (h) Yamamoto, S.; Okujo, N.; Miyoshi, S.-I.; Shinoda, S.; Narimatsu, S. *Microbiol. Immunol*. **1999**, *43*, 993. (i) Yamamoto, S.; Okujo, N.; Yoshida, T.; Matsuura, S.; Shinoda, S. *J. Biochem., Tokyo* **1994**, *115*, 868.

(15) Amin, S. A.; Küpper, F. C.; Green, D. H.; Harris, W. R.; Carrano, C. J. *J. Am. Chem. Soc*. **2007**, *129*, 478.

(16) Gran, G. *Analyst* **1952**, *77*, 661.

(17) (a) Martell, A. E.; Motekaitis, R. J.*The determination and use of stability constants*; Wiley-VCH Inc.: New York, 1992. (b) Gans, P.; Sabatini, A.; Vacca, A. *Talanta* **1996**, *43*, 1739.

data were analyzed either graphically using the Schwarzenbach equation[18] or via nonlinear least-squares refinement using the program SPECFIT/32.[19] The final species distribution diagram was plotted using the calculated protonation constants using HySS2006.[17b] UV−vis spectra were recorded on a Cary 50 spectrophotometer and processed with Varian Win-UV software.

EDTA and EGTA Chelate Competition Experiments. The low pH obtained upon mixing iron(III) with a solution of any of the siderophores indicates that a considerable degree of chelate formation occurs prior to the addition of any base. Since only a small fraction of free metal is present, it is difficult to obtain the overall formation constant from titration data directly. Therefore a chelate competition method was used to obtain the desired formation constant. Solutions for the EDTA or EGTA (Aldrich-Sigma) competition measurements were prepared by adding a known quantity of iron stock to a solution containing 100 mM Bis-Tris (pH 6.0) buffer to avoid Fe-EGTA decomposition at higher pH values,[20] 0.100 M NaCl to fix the ionic strength, a constant amount of siderophore, and varying quantities of EDTA or EGTA in excess and allowing them to come to equilibrium in the dark. The attainment of equilibrium was monitored by optical spectroscopy and appeared to be relatively rapid but samples were left for 1 week as a precaution. The concentration of iron siderophore complex was measured by optical spectroscopy using the known extinction coefficients of the Fe-siderophore and EDTA or EGTA. Data were analyzed using the program SPECFIT/32.

Density Functional Theory (DFT) Calculations. Geometry optimizations were carried out on the two possible structures (vide infra) for the high pH form of FeVF using the B3LYP density functional method and two basis sets: (1) LANL2DZ for all atoms, and a mixed basis of cc-pVDZ for the main group atoms and (2) the CEP-121G basis and effective core potential for iron. Basis set superposition introduces an error of 3−4 kcal/mol in the hydrido energy using either basis set, and additional thermal and zero-point corrections were not applied.

Photoproduct Isolation and Characterization. Iron(III)-vibrioferrin was prepared by addition of a standard solution of $FeCl_3 \cdot 6H_2O$ to apo-vibrioferrin at pH 2.5 and left to equilibrate overnight then purified by HPLC in the dark. A Phenomenex Luna 5 μm C18(2) column was used with the following gradient: (A = H_2O/0.1%TFA, B = CH_3CN/0.1%TFA) 0−10% B in 15 min at a flow rate of 5 mL/min and monitoring the eluant at 300 nm. Purified Fe(III)-VF (7.6 mg) was photolyzed under fluorescent light for 4 h at 20 °C. The photolyzed solution was then lyophilized and repurified by HPLC using the same column with the following gradient: (A = H_2O/0.1%TFA, B = CH_3CN/0.1%TFA) 0−3% B in 5 min, 3−12% B in 5 min, 12−25% B in 12 min, 25−50% B in 13 min at a flow rate of 5 mL/min and monitoring the eluant at 210 nm. Purity of the compound was confirmed by analytical reverse phase HPLC. All HPLC fractions were concentrated by lyophilization.

Routine electrospray−ionization mass spectrometry (ESI-MS) was performed on an Agilent LC/MSD Trap XCT Plus mass spectrometer. For high resolution mass measurements a ThermoFinnigan MAT900XL instrument was used (UCSD). NMR experiments (i.e., ^1H, ^{13}C, gCOSY, TOCSY, gHMQC, and gHMBC) were run at 30 °C in D_2O with 0.03% DSS (Aldrich-Sigma) on a Varian 400 MHz NMR spectrometer using standard pulse sequences obtained from the VnmrJ software (v. 2.2c).

Photolysis Kinetics. All photolysis experiments were conducted at 20 °C in either a Thermo 818 Illuminated Incubator with temperature controller and fluorescent lighting (80 μEinstein m^{-2} s^{-1}) or using a mercury vapor lamp (350 μEinstein m^{-2} s^{-1}). All samples were photolyzed in borosilicate glass vessels. Samples illuminated with the mercury vapor lamp were placed in a jacketed cuvette connected to a constant temperature water bath at 20 °C. Solutions were prepared by adding a known amount of standardized $FeCl_3 \cdot 6H_2O$ to a known amount of siderophore (1:2) in the presence of 0.7 M KNO_3 and 50 mM of the appropriate buffer (MES for pH 5.60, and HEPES for pH 8.00). Solutions kept at extreme ends of the pH range did not contain buffers but the initial and final pH values did not change appreciably during the photolysis. BPDS (4,7-di(4-phenylsulfonate)-1,10 phenanthroline $Na_2 \cdot 3H_2O$, Fluka) was added as required prior to exposure to light (Fe:BPDS = 1:4). Samples exposed to light were corrected for nonspecific reduction by monitoring a control kept in the dark at the same temperature.

Catalytic photooxidation of VF was monitored using a Beckman-Coulter Gold 126 analytical HPLC system equipped with a diode array detector (Gold 168). FeVF was prepared as previously described and excess ligand added before the start of the photolysis. After exposure to a mercury-vapor lamp for various times, an aliquot of the reaction mixture was loaded onto a Luna 5 μm C18(2) analytical column and the products separated with the following gradient (A = 0.1% TFA in MQ-H_2O, B = 0.1% TFA in CH_3CN; flow rate = 0.6 mL/min): 3% B in 5 min, 12% B in 10 min, 12% B in 2 min, 0% B in 2 min.

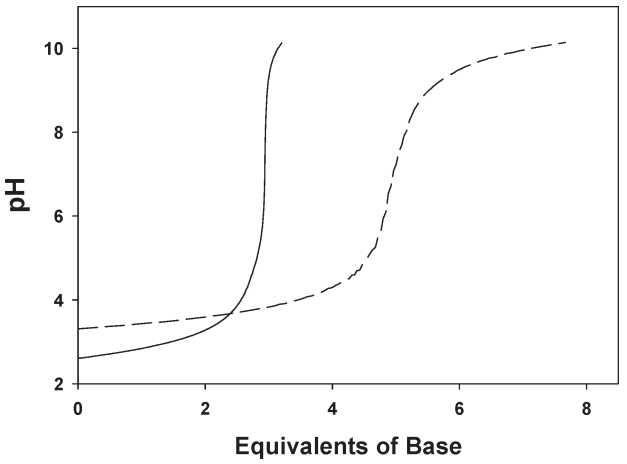

Figure 2. Potentiometric titrations of 0.230 mM VF (solid line) and 0.124 mM Fe(III)-VF (dashed line). Titrations were performed at 25 °C with I = 0.1 M NaCl. The iron complex titration was performed in the dark to avoid photodegradation.

Results

Ligand Protonation Equilibria. The potentiometric titration curve for apo-vibrioferrin is shown in Figure 2. The data below pH 5 and the inflection at 3 equiv of base per mole ligand represents the titration of the three free carboxylic acid groups. Ligand protonation constants were determined from the nonlinear refinement of the data to give evaluated constants (log K_{1-3}) of 5.13(3), 3.60(4), and 2.71(1). These compare well with the corresponding values reported for the related siderophore rhizoferrin (5.25, 4.21, 3.05, and 2.86) which has one additional carboxylate group (Figure 1).[21] Therefore we likewise assign the first protonation constant (pK_a = 5.13) to the free carboxylate of the citrate moiety with the lower

(18) Schwarzenbach, G.; Schwarzenbach, K. *Helv. Chim. Acta* **1963**, *46*, 1390.

(19) Gampp, H.; Maeder, M.; Meyer, C. J.; Zuberbuehler, A. D. *Talanta* **1985**, *32*, 257.

(20) Schröder, K. H. *Acta Chem. Scand.* **1963**, *17*, 1509.

(21) (a) Carrano, C. J.; Drechsel, H.; Kaiser, D.; Jung, G.; Matzanke, B.; Winkelmann, G.; Rochel, N.; Albrecht-Gary, A. M. *Inorg. Chem.* **1996**, *35*, 6429. (b) Silva, A. M. N.; Kong, X.; Hider, R. C. *BioMetals* **2009**, *22*, 771.

two pK_a's of 3.60 and 2.71 assigned to the carboxylic sites of the two α-hydroxy acid moieties.

Metal Ligand Equilibria. The potentiometric titration curve of an equimolar mixture of VF and Fe^{3+} below pH 7 shows a breakpoint at 5 equiv of base (Figure 2) which strongly suggests that, in addition to the three readily titratable carboxylate groups, the two citrate hydroxyl groups are also deprotonated upon iron binding. Between pH 7 and 11 an additional proton is titrated which we assign to the deprotonation of a bound water molecule (vide infra). The potentiometic data over the range of pH from 3 to 11 could be fit using HYPERQUAD with a model that assumed just two metal ligand protonation constants. The evaluated constants were $\log \beta_{110} = 24.03$, $\log \beta_{111} = 28.41$, and $\log \beta_{11-1} = 14.44$.

We initially attempted to derive the $\log \beta_{110}$ value used in the initial fit of the potentiometric metal ligand titration curve from an EDTA competition experiment at near neutral pH, as is standard methodology for siderophores.[9b] However this approach failed in the case of VF as a single equivalent of EDTA effectively removes >95% of the Fe from FeVF. This set an upper limit of between 10^{24} to 10^{25} as a value for K_{ML} or $\beta_{(110)}$. Therefore we sought a weaker chelator whose optical properties were compatible with its analysis in the presence of FeVF. Ultimately we settled on EGTA (Ethylene glycol-bis-(2-aminoethylether)-*N*,*N*,*N*′,*N*′-tetraacetic acid). Using a 2−15 fold excess of EGTA over VF at pH 6.0, it is possible to set up a measurable competition of Fe(III) between the two ligands. The measured equilibrium constant, K_m, of 2.21(9) represents the reaction shown in eq 1:

$$\text{Fe(III)-EGTA} + \text{VF} \rightleftharpoons \text{Fe(III)-VF} + \text{EGTA} \quad (1)$$

where VF and EGTA represent the ligands in all their protonated states. The conditional or pH-dependent formation constant (K^*) for the iron(III)-VF is then given by eq 2:

$$K^*_{FeVF} = K_m K^*_{FeEGTA} \quad (2)$$

which, using the known value of K^*_{FeEGTA},[22] yields a value of 14.57(5) for $\log K^*_{FeVF}$ at pH 6.0. While this is a valid equilibrium constant under the conditions for which it is measured, it is difficult to compare with the "standard" pH-independent stability constants typically reported which are expressed in terms of the fully deprotonated form of the free ligand. This calculation in turn requires knowledge of the ligand deprotonation constants. Unfortunately only three of the five required deprotonation constants could be determined for VF since the pK_a's of the two citrate hydroxyl groups were not measurable by potentiometric titration at the concentrations of ligand available. If, however, we estimate the values for these two deprotonations as 10.1 and 11.3 (using the dicitrate siderophore rhizoferrin as a model),[21] we can estimate the pH-independent stability constant. Given these estimates the overall formation constant, $\log K_{ML}$, for the Fe(III)-VF complex is then determined to be 24.02(5), a value that is unusually small for a

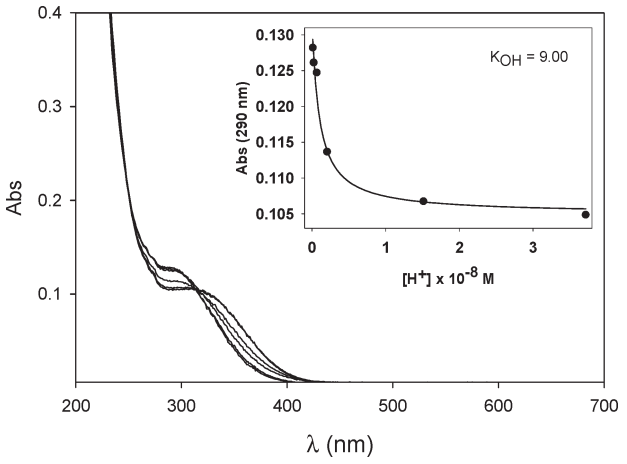

Figure 3. Spectrophotometric titration of Fe(III)-VF from pH 7.43−9.96. Experiment was performed in the dark at 25 °C with I = 0.1 M NaCl. Inset: Schwarzenbach fit of the spectrophotometric titration in the indicated pH range yielding $\log K_{OH} = 9.0$ ($R^2 = 0.97$).

confirmed siderophore and somewhat less than that of the related siderophore rhizoferrin (Figure 1) which has $\log K_{ML} = 25.3$.[21a] This is presumably the result of VF having one fewer donor group than rhizoferrin. The proposed coordination for Fe(III) to VF involves ligation by both hydroxyl groups and the three carboxylates analogous to the proposed coordination of Fe(III) by rhizoferrin with the sixth coordination site presumably occupied by a water molecule. A similar coordination scheme has been proposed by others.[23]

Spectrophotometric Titration. At pH values above 7.8 a progressive blue shift and an increase in intensity of the oxygen-to-iron LMCT band of the complex near 330 nm indicates a significant change in the inner coordination sphere. Such changes can be assigned to the deprotonation of the aqua ligand to yield the hydrolyzed species:

$$[\text{FeL(H}_2\text{O)}]^{2-} \rightleftharpoons [\text{FeL(OH)}]^{3-} + \text{H}^+ \quad (3)$$

An alternate structure, which involves deprotonation and coordination of an amide group to the iron as seen in some iron enzymes such as nitrile hydratase, was also considered.[24] However, DFT calculations indicate that the optimized hydroxo form is 27−34 kcal/mol (depending upon basis set used) more stable than the amido plus water formulation indicating that the latter was highly unlikely. Therefore this process was fit to the simple single proton Schwarzenbach equation,[18]

$$A_{obs} = (A_{MHL}K[\text{H}^+] + A_{ML})/[\text{H}^+]K + 1$$

where in general A_{obs} is the observed absorbance, A_{MHL} the absorbance due to the protonated species, A_{ML} that of the unprotonated, and K the equilibrium constant between them. This analysis yields a hydrolysis constant, $\log K_{OH}$ of 9.0 (Figure 3). Such a value is consistent with expectations for a Fe(III)-siderophore with an overall binding constant in the range of 10^{23-27} as there is typically a linear correlation between the overall formation constant of an iron complex

(22) Martell, A. E.; Smith, R. M. *Critical stability constants*; Plenum Press: New York, 1974.

(23) Budzikiewicz, H. *Mini-Rev. Org. Chem.* **2005**, *2*, 119.

(24) Murakami, T.; Nojiri, M.; Nakayama, H.; Odaka, M.; Yohda, M.; Dohmae, N.; Takio, K.; Nagamune, T.; Endo, I. *Protein Sci.* **2000**, *9*, 1024.

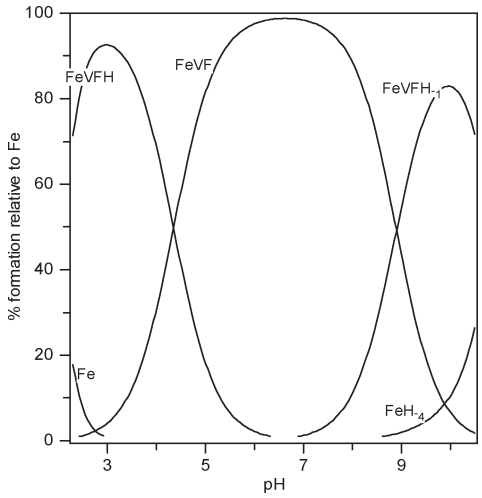

Figure 4. FeVF species distribution as a function of pH using protonation constants obtained from SpecFit/32. Species distribution was constructed using HySS2006.

Table 1. Deprotonation Constants for the FeVF Complex[a]

species	Hyperquad	Specfit	Schwarzenbach
log $K_{(MH_{-1}L)}$	9.59	8.90	9.00
log $K_{(ML)\ fixed}$	24.03	24.03	
log $K_{(MHL)}$	4.38	4.35	4.40

[a] Values were extracted via a global fit to the data using SpecFit/32, stepwise fits to the Schwarzenbach equation, or fits to the potentiometric titration using Hyperquad.

and its first hydrolysis constant.[25] Between pH 7.8 and 3.5 only minor changes in the LMCT band intensity and position were evident indicating no major change in the coordination sphere of the Fe^{3+}. Attempts to fit this region to a single protonation equilibrium via Schwarzenbach analysis gave a log K of 4.40. The minor spectral changes in the LMCT band over this pH range suggest an equilibrium that involves protonation of the terminal carboxylate group rather than the α-hydroxy acid moieties. At pH values lower than 2, a dramatic reduction in the intensity of the LMCT band indicates dissociation of the complex in this pH regime. Using the program SPECFIT/32 we were able to construct a global model that satisfactorily accounts for the distribution of various FeVF species over the pH regime from 2 to 10 (Figure 4). The constants derived from this global model are given in Table 1, and the calculated spectra for individual species are provided in the Supporting Information, Figure S3. In general there is fair agreement between the values obtained by global refinement of the spectrophotometric titration data, the stepwise Schwarzenbach analysis, and the fits to the metal−ligand potentiometric titration (Table 1).

Photochemistry. As expected for a siderophore containing two α-hydroxy acid units, FeVF was found to be photolabile producing an oxidized ligand photoproduct with concomitant reduction of Fe(III) to Fe(II). Photolysis of Fe(III)-VF by natural sunlight (1500 μEinstein $m^{-2}\ s^{-1}$) was monitored by ESI-MS in both positive and

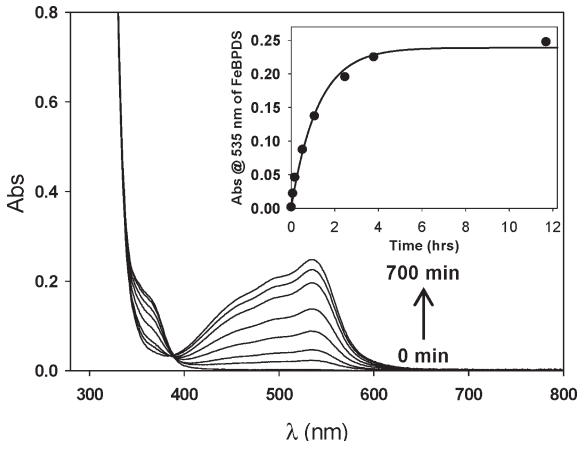

Figure 5. Photolysis of FeVF over 700 min upon exposure to a fluorescent light source in the presence of the Fe(II)-chelating agent, BPDS, at pH 2.9, 20 °C and I = 0.7 M KNO_3. Inset: Single exponential fit of $Fe(BPDS)_3$ absorbance at 535 nm vs time (R^2 = 0.99).

negative ion modes which gave qualitatively similar results. In negative ion mode, prior to photolysis only peaks corresponding to free VF (433 amu) and its iron complex (486 amu) are seen. Over the course of an hour the peaks corresponding to VF and FeVF are seen to diminish in intensity while new peaks grow in at 389 and 442 amu which correspond to VF* and FeVF*.[26] After 2 h only the peak due to free VF* photoproduct remains.

Kinetics of Photolysis. In comparison to other photoactive marine siderophores such as petrobactin, aerobactin, the aquachelins, or the marinobactins, FeVF proved exceptionally susceptible to photolysis.[7,9b,27] For example, when exposed to a mercury-vapor lamp >95% of a 0.1 mM solution of Fe(III)-VF photolyzes within 6 min. Even in the presence of a 1000-fold excess of ligand, 20 min of exposure to light resulted in the complete photooxidation of all of the VF, as indicated by the disappearance of the corresponding peak in the HPLC. Thus, to prevent excessive photolysis and to obtain easily measurable reaction rates, we moved from a mercury vapor lamp to standard fluorescent lighting as an energy source. We initially monitored the rate of photolysis by measuring the disappearance of the 330 nm LMCT band of FeVF as a function of time. However, this band has a low extinction coefficient that required high concentrations of VF (a product obtained in low yield). Hence we conducted further experiments in the presence of the Fe(II) trapping agent BPDS and used the large extinction coefficient of $Fe(BPDS)_3$ absorbance band at 535 nm to monitor the photolysis.[28] Under similar conditions the rate constants measured by the two procedures were equivalent within experimental error (Supporting Information, Table S1), indicating that the presence of the trapping agent did not appreciably affect the rate of photolysis and thus all subsequent experiments were conducted in the presence

(25) Harris, W. R.; Carrano, C. J.; Raymond, K. N. *J. Am. Chem. Soc.* **1979**, *101*, 2722.

(26) Although an FeVF* complex is observed in the ESI-MS, we believe this is a byproduct of the ionization method representing anionic-cationic interactions and not a "real" iron complex. Further evidence can be found in ref 33.

(27) (a) Barbeau, K. *Photochem. Photobiol.* **2006**, *82*, 1505. (b) Barbeau, K.; Rue, E. L.; Trick, C. G.; Bruland, K. W.; Butler, A. *Limnol. Oceanogr.* **2003**, *48*, 1069.

(28) Cowart, R. E.; Singleton, F. L.; Hind, J. S. *Anal. Biochem.* **1993**, *211*, 151.

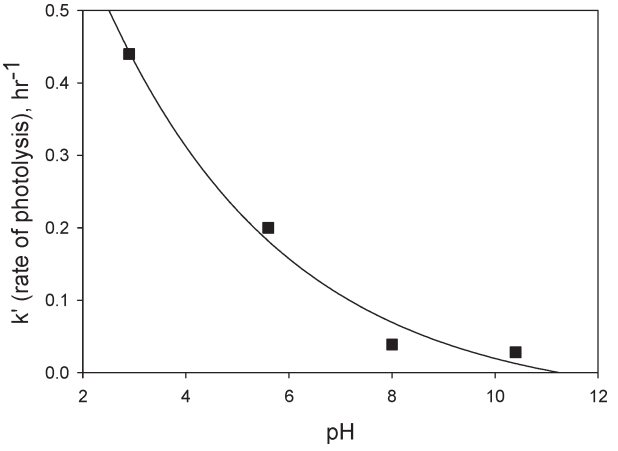

Figure 6. Rate constants for photolysis of FeVF as a function of pH. Duplicate experiments were performed at 20 °C with I = 0.7 M KNO_3 using fluorescent light as the energy source. Error bars were not shown when smaller than the symbol.

of BPDS. Clean first order kinetics and tight isosbestic points were observed indicating the presence of only two absorbing species during the photolysis (Figure 5). The reaction rate constant was seen to decrease rapidly as a function of pH (Figure 6) so that at the acidity of seawater (pH 8.0) the photolysis of FeVF had a half-life of 17.7 h while petrobactin or the peptidic portion of the marinobactins showed no observable (< 5%) photolysis under the same conditions.

Structure Elucidation. Having observed that FeVF was very susceptible to photolysis we sought to determine the structure of the photoproduct, VF*. The lack of any apparent appreciable affinity for Fe(II) or Fe(III) by the photoproduct (as indicated by the complete loss of the LMCT band and the negative CAS response of VF*) allowed for its simple isolation by HPLC without the need to extract the iron. Complete structural characterization was obtained by a combination of mass spectral and NMR methods.

The sodium adduct of the photoproduct has an exact mass of 411.1019 (difference between measured and theoretical mass of 411.1010 amu, Δ = 2.2 ppm) which gives a molecular formula for the $[M + Na]^+$ ion of $C_{15}H_{20}O_{10}N_2Na$. The most characteristic feature of the ^{1}H NMR of VF* is its extreme simplification in comparison to VF itself because several protons lose their diastereotopic nature.[14i] The presence of single sharp methyl doublet from the alanine residue at 1.47 ppm indicates there is only a single form of VF* unlike VF which displays two such doublets in an about 2:1 ratio because of the presence of open and closed chain forms (Figure 7, Supporting Information, Figure S1). Another important feature is the simplification of the citrate region in VF* compared to VF. The latter contains two distinct sets of diastereotopic protons, integrating to four protons each, for the two distinct citrate groups in the molecule while the former contains only a single ABX_2-type system integrating to four protons, centered at 2.89 ppm, assigned to the diastereotopic citrate protons (H-2ab, H-4ab) (Supporting Information, Figure S1). The chemical shift values indicate that it is the terminal citrate group that is retained while that associated with the 2-ketoglutarate derived five-membered ring is lost. This is corroborated by the presence of a sharp singlet integrating

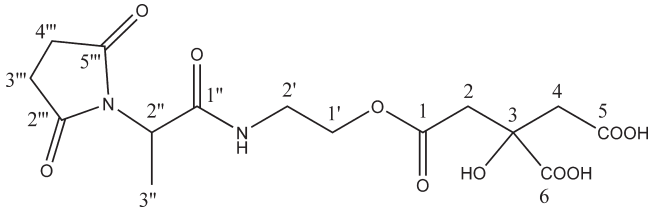

Figure 7. Proposed structure of the major photoproduct of vibrioferrin, VF*.

Table 2. ^{1}H and ^{13}C Chemical Shift Assignments for VF* in D_2O (0.03% DSS)

^{1}H δ (ppm) in D_2O	assignment
1.47 (d, 7 Hz)	H-3″
2.79 (s)	H-3‴, H-4‴
2.77−2.84 (m)	H-2a, H-4a
2.95−3.02 (m)	H-2b, H-4b
3.48 (m)	H-2′
4.17 (t, 5 Hz)	H-1′
4.78 (q)	H-2″
^{13}C δ (ppm) in D_2O w/DSS	**assignment**
14.11	C-3″
29.13	C-3‴, C-4‴
39.47	C-2′
44.44	C-2
44.49	C-4
50.15	C-2″
64.40	C-1′
74.59	C-3
172.43	C-1
172.55	C-1″
174.85	C-5
178.39	C-6
181.46	C-2‴, C-5‴

to four protons corresponding to H-3‴ and H-4‴ centered at 2.79 ppm and further shows that the five-membered ring has 2-fold symmetry (Figure 7, Table 2). The ^{13}C NMR spectrum shows the presence of only 13 sharp resonances as compared to 16 seen in VF (Supporting Information, Figure S2). The most characteristic feature is the disappearance of one of the quaternary carbons of VF (91.9 ppm) because of the loss of CO_2 from the five-membered ring. The carbonyl region shows only five signals, rather than the six seen in VF, with one roughly twice the intensity of the others assignable to the two equivalent succinimidyl carbonyls on the ring (C-2‴ and C-5‴). In addition only six, rather than seven, methylene carbon resonances are seen in VF*, again one of which is twice the intensity of the others, assignable to the two equivalent methylenes of the five-membered succinimidyl ring (C-3‴ and C-4‴). The proposed structure is shown in Figure 7 and complete assignments, verified by the appropriate 2-D experiments, are given in Table 2.

Discussion

Vibrioferrin is a member of the carboxylate class of siderophores containing two α-hydroxy acid groups originally isolated from *V. parahemolyticus*, an enteropathogenic estuarine bacterium often associated with seafood-borne gastroenteritis.[14a,d,e,i] Previously, we isolated VF from two specific clades of *Marinobacter* species.[15] These clades are a unique subset of bacteria which have been found to be specifically associated with bloom-forming dinoflagellates

Table 3. pM Values for Various Fe(III)-Siderophore Complexes[a]

complex	pM_1	pM_2
Rhizoferrin[b]	19.7	
Aerobactin[c]	23.3	
Petrobactin[d]	23.0	
Marinobactin E[e]	25.8	27.5
Vibrioferrin[f]	18.4	19.6

[a] $pM_1 = -\log [Fe^{3+}]$ where $[L]_0 = 10^{-5}$ M, $[Fe]_0 = 10^{-6}$ M, and pH = 7.4. pM_2 pH 8.0. pM values are based on published stability constants (see references in footnotes b−f). [b] Ref 21a. [c] Ref 25. [d] Ref 9a. [e] Zhang et al., submitted for publication. [f] This work.

including toxic species such as *G. catenatum* isolated from places as far apart as the Pacific and Atlantic oceans. This functional conservation is interpreted as indicating that there are specific selective processes operating between the bacterium and dinoflagellate.[29] Why are dinoflagellates selecting for such a phylogenetically and functionally specific group of marine bacteria? Can we find any clues in the unique features of vibrioferrin as to the nature of this and related algal-bacterial relationships?

The first obvious feature unique to VF is its relatively weak iron binding properties. This is presumably a direct result of the fact that VF lacks the six donor groups required to complete the octahedral coordination geometry preferred by Fe(III) and generally found in other siderophores. While it is difficult to compare the overall formation constants of iron chelators to one another because of differences in ligand pK_a's and/or stoichiometry, the "pM" value has been proposed as a means for more direct comparison.[25] The pM values express the amount of "free iron" present at equilibrium under particular sets of experimental conditions, typically at a total ligand concentration of 10^{-5} M, a total iron concentration of 10^{-6} M, and a pH of 7.4 (Table 3). It is clear that vibrioferrin is not a particularly powerful iron chelator as compared to the more usual tris(hydroxamate) or tris(catecholate) or mixed ligand siderophores at this pH.[30] For example petrobactin and marinobactin E, siderophores known to be produced by closely related, but nonalgal associated, *Marinobacter* spp., are 10^4 to 10^7 fold better chelators than VF, a difference that only increases at the higher pH value of seawater.

Beyond its relatively weak Fe(III) binding, the most remarkable feature of VF is the striking sensitivity of its iron complex to photolysis. Similar to citrate, the iron complexes of siderophores that contain a α- or *β*-hydroxy acid moiety are generally photosensitive and undergo photolysis causing the loss of a carboxylate group from the ligand in the form of CO_2 and the concomitant reduction of the metal and its release as Fe(II). Although the exact mechanism for the photochemical degradation of iron citrate is complex, the reduction of Fe(III) and radical anion generation are generally observed.[31] It is perhaps significant that most of these hydroxy acid-containing siderophores seem to be associated with the marine environment.[32] However, the photoproducts formed from the photolysis for all the siderophores studied thus far have been found to retain the ability to coordinate Fe(III) so that the overall photolysis reaction is actually that shown in eqs 4 and 5.[7,9]

$$\text{Fe(III)-Sid} + h\nu \rightarrow \text{Sid}^* + \text{Fe(II)} \quad (4)$$

$$\text{Sid}^* + \text{Fe(II)} + O_2 \rightarrow \text{Fe(III)-Sid}^* \quad (5)$$

Indeed in some cases the photoproduct (sid*) is actually a *better* Fe(III) chelator than the parent siderophore![9] It has also been shown in the one case where it was studied that the Fe(III) complex of the photoproduct is recognized by the bacteria that produce the parent siderophore and is taken up via the same transport system with equal affinity.[9b] In light of these observations, we anticipated that FeVF would also be photosensitive and undergo photooxidation containing as it does two α-hydroxy acid moieties. FeVF did indeed undergo photolysis, and at a faster rate under relatively low illumination conditions than other photoactive siderophores, to produce a monodecarboxylated photoproduct and Fe(II).[33] What was unanticipated was the fact that the resulting photoproduct has *no* significant affinity for Fe(III). Thus the photolysis of Fe(III)-VF is an irreversible process that leads to the destruction of the siderophore and the ultimate formation of "free" Fe(III) as in eqs 6 and 7

$$\text{Fe(III)-VF} + h\nu \rightarrow \text{VF}^* + \text{Fe(II)} \quad (6)$$

$$\text{Fe(II)} + O_2 \rightarrow \text{Fe(III)}' \rightarrow \text{Fe(III)}\downarrow \quad (7)$$

where Fe(III)′ represents transiently soluble iron hydroxo species and Fe(III)↓ represents the increasingly insoluble mineral phases present at equilibrium.

Unlike other photosensitive siderophores where the photoproduct retains the ability to coordinate and sequester Fe(III), the lack of affinity for iron of the photoproduct of VF leads to catalytic destruction of the ligand (Scheme 1). With such a rapid turnover rate, it appears that even trace amounts of Fe(III) will eventually consume a large excess of VF under high light flux conditions. Such a scenario seems to be metabolically wasteful in the extreme until one notes that the Fe(II) formed by the photolysis of Fe(III)-VF is expected to be rapidly oxidized to Fe(III) under seawater conditions.[34] The Fe(III) thus produced is initially in the form of relatively soluble simple hydroxo complexes (Fe(III)′) which are only slowly converted into the more refractory oxo-hydroxo polymeric mineral phases. Using ^{55}Fe-labeled VF we have shown that the soluble iron pool, that is, Fe(III)′ initially produced after aerobic photolysis is in fact more rapidly and efficiently taken up by the producing bacteria than that of intact Fe(III)-VF itself.[33] Equally significant is the fact that associated phytoplankton are also more capable of assimilating ^{55}Fe generated from photolyzed Fe(III)-VF than from intact Fe(III)-VF by more than an order of magnitude.[33] In view of these findings, we propose that VF photodegradation may be an evolutionarily adapted function by which the producing bacteria "share" the soluble, photochemically produced iron with their algal associates possibly in exchange

(29) Green, D. H.; Llewellyn, L. E.; Negri, A. P.; Blackburn, S. I.; Bolch, C. J. S. *FEMS Microbiol. Ecol.* **2004**, *47*, 345.
(30) Harris, W. R.; Raymond, K. N.; Weitl, F. L. *J. Am. Chem. Soc.* **1981**, *103*, 2667.
(31) Abrahamson, H. B.; Rezvani, A. B.; Brushmiller, J. G. *Inorg. Chim. Acta* **1994**, *226*, 117.
(32) Butler, A. *BioMetals* **2005**, *18*, 369.
(33) Amin, S. A.; Green, D. H.; Hart, M. C.; Kuepper, F. C.; Sunda, W. G.; Carrano, C. J. *Proc. Natl. Acad. Sci. U.S.A.* **2009**, *106*, 17071−17076.
(34) Morgan, B.; Lahav, O. *Chemosphere* **2007**, *68*, 2080.

Scheme 1. Fe Catalyzed Photochemical Oxidation of VF

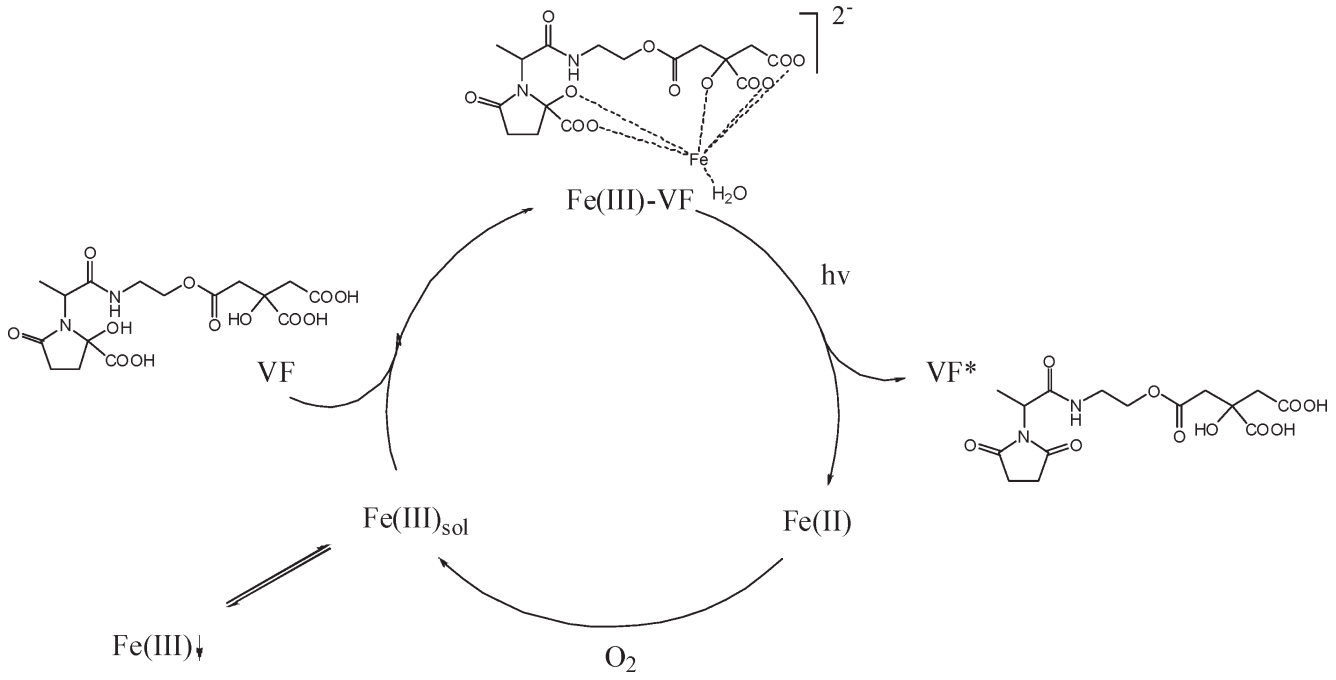

for algal-excreted metabolites. Work designed to further address this hypothesis is underway.

Acknowledgment. This work was supported by NOAA Grants NA04OAR4170038 and NA08OAR4170669, California Sea Grant College Program Project numbers R/CZ-198 and R/CONT-205, through NOAA's National Sea Grant College Program, U.S. Dept. of Commerce. The authors would like to thank Andrew Cooksy (SDSU) for the DFT calculations.

Supporting Information Available: ^{1}H and ^{13}C NMR spectra of the vibrioferrin photoproduct, photolysis rate constants as a function of pH, calculated spectra for the various species identified in the spectrophotometric titration, and complete author list for references 11a and 11b. This material is available free of charge via the Internet at http://pubs.acs.org.